Analysis of Erosion and Redeposition Processes in Coaxial Vacuum Arc Thrusters

IEPC-2019-661

Presented at the 36th International Electric Propulsion Conference
University of Vienna, Austria
September 15-20, 2019

Matteo Laterza* and Igal Kronhaus†
Faculty of Aerospace Engineering, Technion, Technion City, Haifa, 320003, Israel

Vacuum arc thruster erosion processes are characterized using several sets of electrode interface geometries in an actively fed coaxial vacuum arc thruster. In each set, the thruster is operated until failure whereas the electrode interface geometry, between anode, cathode and insulator, is periodically inspected using laser profilometry and microscope imagery. Thrust and power measurements of the thruster were recorded as well. It was found that the most common failure event is a short circuit due excessive redeposition of cathode material as a conductive layer on the insulator. A preferable combination of interface geometry, cathode feeding rate, and arc current is found. This specific combinations enables prolonged thruster operation processing at least 1 gram of cathode material.

List of Acronyms

APB	= amplified piezo brake
BN	= boron nitride
ISF-VAT	= inline screw feeding vacuum arc thruster
PM	= propulsion module
PPU	= power processing unit
PS	= power supply
VAT	= vacuum arc thruster

*Postdoctoral Fellow, Aerospace Plasma Laboratory, laterza.matteo@gmail.com .
†Head, Aerospace Plasma Laboratory, kronhaus@technion.ac.il .

I. Introduction

Vacuum arc thrusters (VAT) are promising propulsion devices for nano-satellites and CubeSats,[1,2] with a few examples experimentally operated in space. VAT are pulsed-dc devices that utilize arc discharge, across an insulator, between two electrodes to produce thrust. The main advantages of the VAT compared to other electric propulsion devices is in its simplicity and scalability to very low power ($< 10W$). In a VAT the cathode electrode is consumed as propellant during the discharge. The cathode is eroded in localized regions, where the discharge is attached, known as "cathodic spots".[3] The metal plasma emitted from these micrometer sized spots is naturally accelerated by gasdynamic expansion.[4] Further acceleration of the plasma plume can be achieved by the use of a magnetic nozzle.[5,6]

Significant technical development of these devices was made by several groups in the last decade. There are two established configuration: co-axial and the ring shaped,[7] termed according to the shape and placement of the cathode with respect to the anode. As any rocket it is important maintain controlled feeding of the propellant in the VAT during its operating life time. Recently a co-axial VAT was developed with an active, fully controlled, feeding mechanism known as the inline-screw-feeding VAT (ISF-VAT).[8,9] In this paper we analyze the processes determining the ISF-VAT life time: namely erosion of the electrodes and insulator as well as plasma metal deposition.

II. Thruster and Experimental Setup

A. Thruster Setup

The patented ISF-VAT concept,[10] shown in Fig. 1, is a co-axial vacuum arc thruster with active feeding mechanism. A central cathode rod is freely disposed within a concentric insulator tube. A second electrode, positioned at the outer edge of the insulator, functions both as the anode of the dc circuit and as the exit plane of the thruster. To keep the VAT geometry constant during long duration operations, the cathode, connected to a metallic headless screw, is advanced at a precise rate inside the insulator in a helical path. The screw provides also an electrical contact with the thruster body that is under negative potential. With the correct selection of the linear advance rate and screw pitch, a balance between cathode erosion and feeding can be achieved. The helical motion both compensates for the radial as well as the azimuthal cathode erosion patterns. This allows for constant thruster geometry throughout the operational life of the thruster as well as improved uniformity of the recoating process, i.e. the process of replenishing the conducting layer on the cathode-insulator-anode interface.

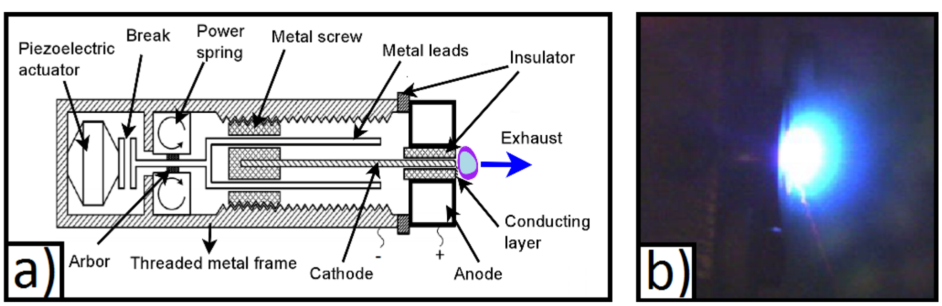

Figure 1. Schematics of the ISF-VAT thruster (a) and thruster plume during operation (b).

To keep power consumption and thruster dimensions to a minimum, as shown in Fig. 1 (a), a mechanism comprised of a spiral spring and an amplified-piezoelectric-actuator (APB) was chosen to power the cathode rotation. The mechanical energy is stored in the spring, and the APB regulates the spring unwinding motion. Figure 1 (b) shows the thruster plume during operation, as recorded by a CCD camera.

The experiments were performed on a ISF-VAT propulsion module (PM) that is being developed at the aerospace plasma laboratory (APL), Technion.[8,9] The PM includes two ISF-VATs, a power processing unit (PPU), and a structural frame to interface the module with a standard cubesat bus. In addition to generating the discharge the PPU also powers the propellant (cathode) feeding mechanism. Figure 2 (a) shows a photograph of the PM. This PM contains only one ISF-VAT and has a modified frame for easy interference with APL's thrust balance system.

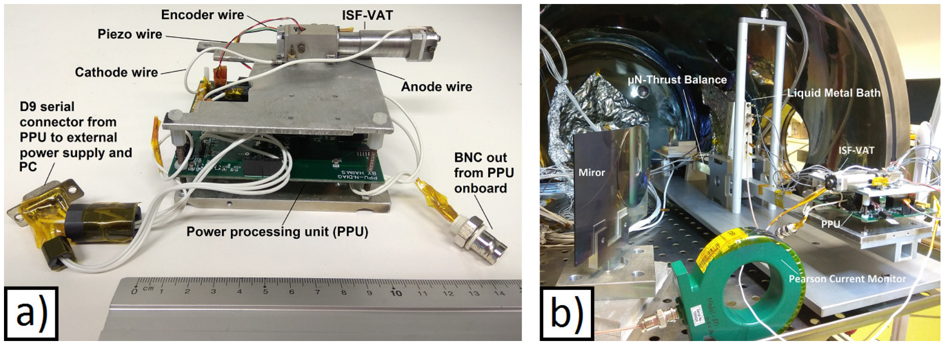

Figure 2. Photgraph of the laboratory PM (a), and the PM installed on a thrust balance in the vacuum chamber (b).

B. Experimental Setup

The experiments were conducted in APL's vacuum chamber. The vacuum chamber dimensions are 0.6 m diameter a length of 1.2 m. During thruster operation the pressure is maintained $< 10^{-5}$ mbar by a set of turbopumps with a pumping speed of 1200 l/s. Figure 2 (b) shows the placement of the PM onto the thrust balance and the feedthrough electrical connections in the vacuum chamber.

1. Power Measurements and Control System

Figure 3 shows a diagram of the PPU and power measurement system for the thruster placed inside the chamber. To enable long duration tests of the ISF-VAT a requirement was put to run experiments automatically without human supervision. The main concern is detecting a short circuit failure of the thruster and eanbling immediate shut down ($<$ 1 sec) in such event. An additional requirement was to record the input current to the PPU continuously during the test.

A Labview program, running on a personal computer, was developed to provide automatic control over the test. This program is able to remotely control a DC power supply (PS) that powers the PM, through a LAN. Its features include control over PS voltage and enable/disable of over-current protection. The program also has the ability to record the PPU input current. The current is measured by a Tektronix A622 Hall current monitor that converts it to a voltage signal. This signal is sampled by an analog to digital converter (National Instruments, USB-6216) that is attached to the computer. The PS voltage was 16 V. The system can measure 200 ks/s. However, typically, a sampling (averaging) time of 0.5 s is used for the current measurement. This enables easy synchronization with the output signal of the thrust balance (also with 0.5 s integration time). The input power measurement is also use to detected shorts. To compute the efficiency of the PPU the output current was also measured through a Pearson Current Monitor model 150 installed directly inside the vacuum chamber. Arc current measurements were recorded using a Tektronix MDO 3104 oscilloscope with a 1 GHz frequency and a 5 GS/s sampling density. Discharge voltages are measured using a differential voltage probe.

Thrust measurements were performed using a commercial torsion balance (FOTEC)[11] with an accuracy of $\pm 0.2\mu N$. The system consists of two balanced arms connected to the frame through a magnetic bearing and a torque spring. At the end of each arm are positioned two horizontal plates, one for the thruster and the other for balancing weights. Electrical connections are passed through a liquid gallistan bath placed on the axis of rotation, to minimize parasitic torque. Two different sets of measurements are performed to determine thrust. The first measurement is an optical displacement measurement, that combined with information on the spring rate allows to compute the torque and then the applied force. An electrostatic force actuator is also provided. The actuator can be used both to calibrate the spring rate and to keep the relative displacement near zero, thus minimizing the impact of the spring non-linearity.

C. Electrode Interface Inspection

The thruster was inspected at several times both before and after termination of operation as well as at several points in between. The inspection process is non-invasive but required the removal of the thruster

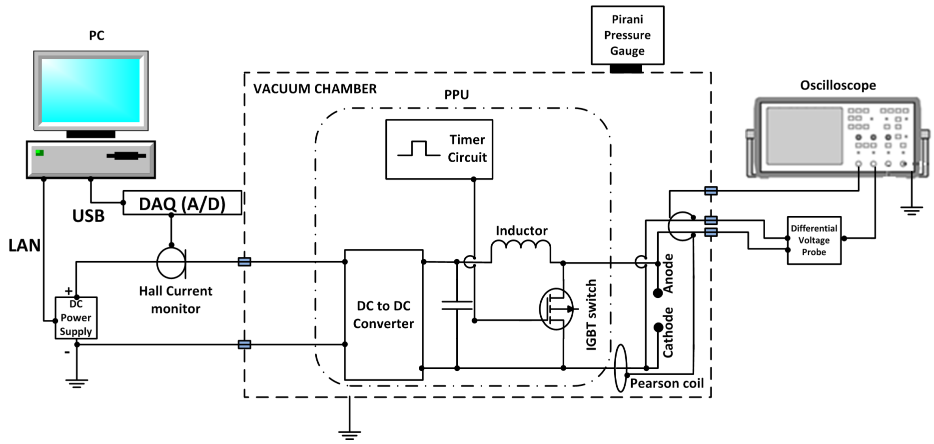

Figure 3. Electrical scheme of the PPU (excluding feeding system) and current measurement system.

from the chamber. The thruster was placed vertically on a custom stand, and a picture of the thruster head was taken with a microscope at 40X magnification with a 1.3MP CCD camera. The surface profile of the cathode-insulator-anode was scanned by a laser profilometer (Keyence LJ-V7020). The scan is performed on a line 35 μm wide and 15 mm long. The sampling interval along the line is 10 μm and the repeatibility in the vertical direction is 0.2 μm. After this operation the thruster was returned to the chamber to continue the experiment. Figure 4 shows a diagram of the thruster head and the taken measurements, to be used as a reference for the figures in next chapter.

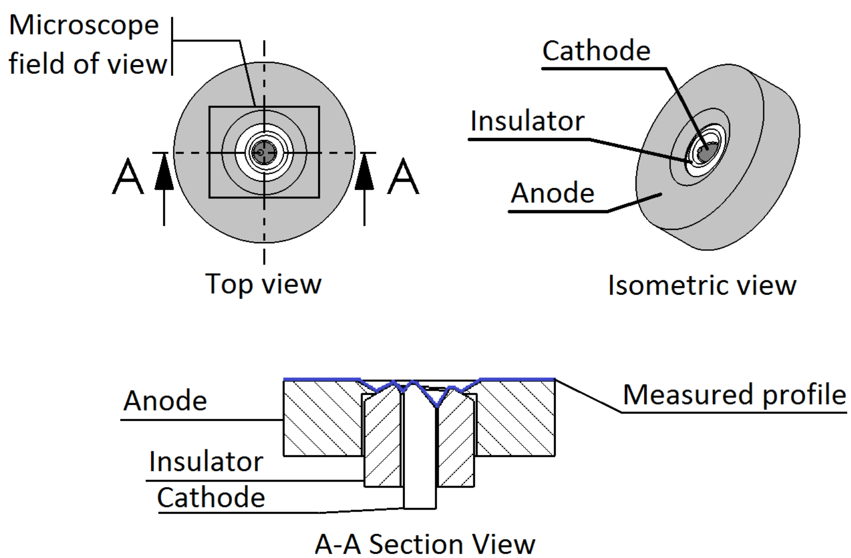

Figure 4. View of microscopy and profilometry measurements.

D. Experimental Procedure

Before thruster operation, profilometry is performed on the electrode interface to measure its initial state. This serves as a reference for tracking the interface evolution during the experiment. A graphite coating is then placed on the insulator surface. The thruster is then attached to the PM and the PM itself is installed on the thrust balance.

The operating cycle of the PM is divided in three parts: firing, cathode advancing, and cool down. The thruster firing stage consists in short 200-400 us second pulses fired at a frequency of 15 HZ. Figure **??** shows a typical measured current-voltage characteristic of an individual arc pulse.

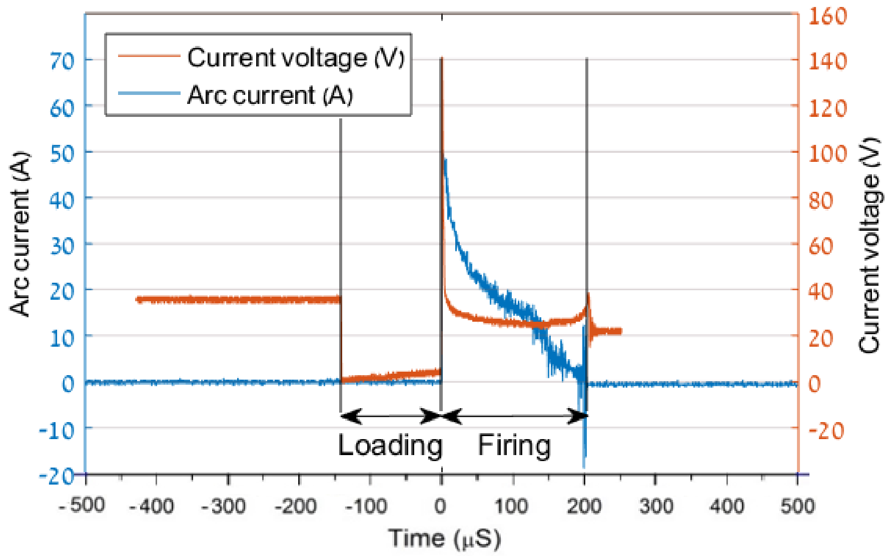

Figure 5. I-V characteristic of a single pulse of arc discharge.

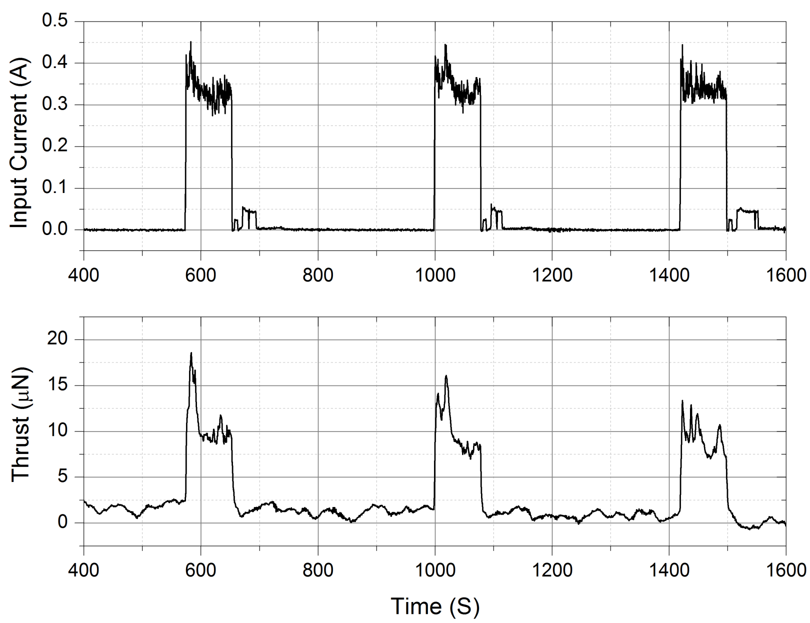

Figure 6. Characteristic thrust and input current measurements during PM operation.

The firing is controlled by an internal dedicated timing circuitry. The duration of a single firing stage is 90 s. After the firing stage is completed, the feeding system is activated to complete a cathode advance of 1/12th of a turn, corresponding to 62 μm. After a cool down phase the cycle is repeated. Figure 6 shows the PPU input current and thrust measurements highlighting the different phases of the cycle. The lifetime of the thruster is measured in the number of turns of the screw. In many cases the thruster reaches its end of life with an electrical short, when the insulator erosion and plasma deposition forms a path of direct contact between the cathode and the anode.

III. Results and Discussion

Using the PM and experimental setup, four cases of electrode interfaces were evaluated. The main parameters tested are insulator geometry, insulator material, and peak arc current.

A. Flat alumina insulator, 40 A peak discharge current

The thruster failed with a short circuit after 4.5 turns. Photographs of the thruster surface are shown in Fig. 7. Profilometry results of the thruster surface is provided in Fig. 8.

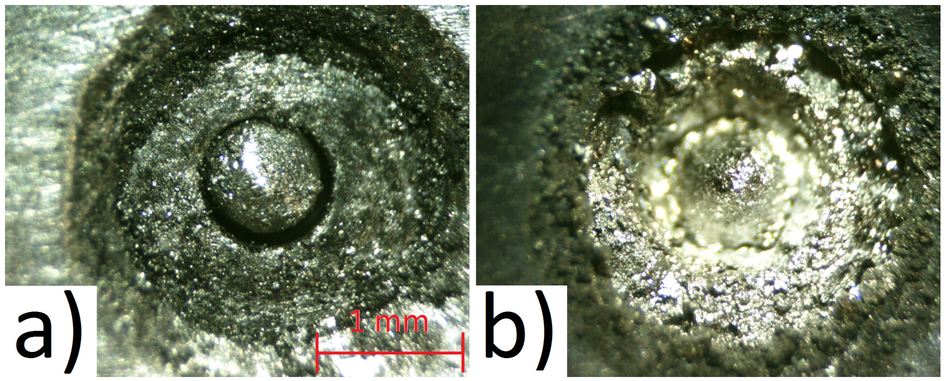

Figure 7. Photograph of a flat alumina insulator, operated at 40 A peak discharge current, taken at 0 turns (a) and 4.5 turns (b). The images show a coaxial structure with the cathode in the center insulator in the middle and metal anode.

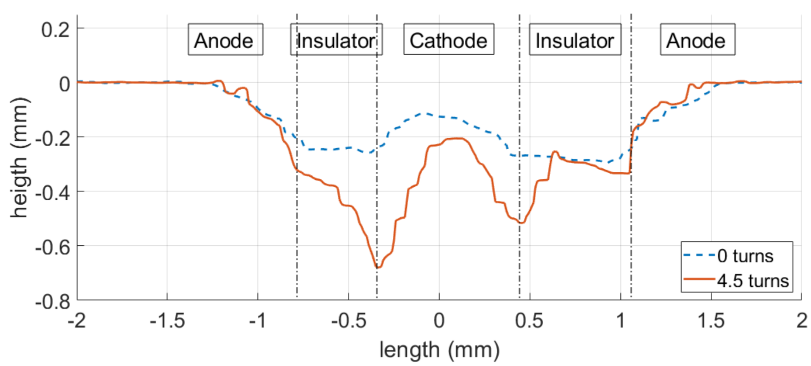

Figure 8. Laser profilometry results for the flat alumina insulator, operated at 40 A peak discharge current, showing the anode-insulator-cathode surface. 0 and 4.5 turns. Axes not to scale.

B. Conical alumina insulator, 40 A peak discharge current

The thruster failed with a short circuit after 6 turns. Photographs of the thruster surface are shown in Fig. 9. Profilometry results of the thruster surface is provided in Fig. 10.

Although both cases (A and B) terminated with a short circuit, the cone shaped insulator (case B) operated for longer before failing. Comparing the surface profiles of the flat and conic alumina insulator, it can be seen that in both cases the insulator eroded around the cathode by ≈ 0.3 - 0.4 mm. The anode erosion in both cases is negligible. However, Fig. 7 and 9 significant exhibit significant metal deposition on the anode and insulator surfaces. The depositions grow toward each other until a short circuit is created. This process explains why the conical insulator is more resistant. In the case of the flat alumina the cathode is recessed and the plasma plume forms inside the interface enabling fast deposition on the insulator-anode interface, whereas in the conical case the cathode is initially flush with the anode ejecting less material toward the insulator-anode interface, the eroded insulator also forms a double-cone structure that reduces the plasma flux to the anode-insulator interface.

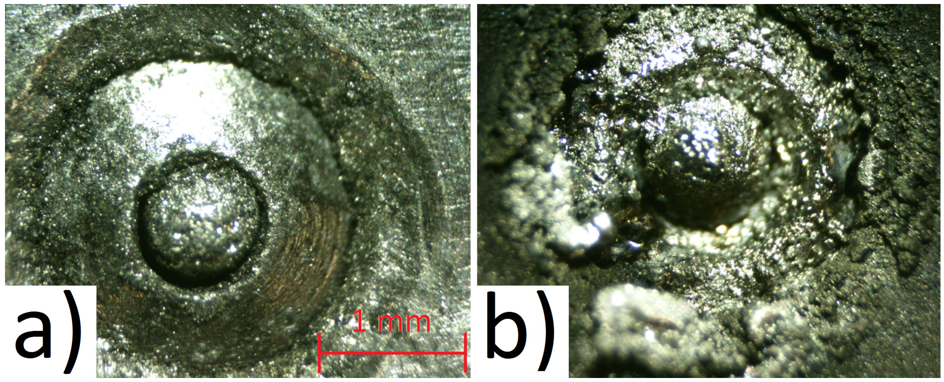

Figure 9. Photograph of a conical alumina insulator, operated at 40 A peak discharge current, taken at 0 turns (a) and 6 turns (b). The images show a coaxial structure with the cathode in the center insulator in the middle and metal anode.

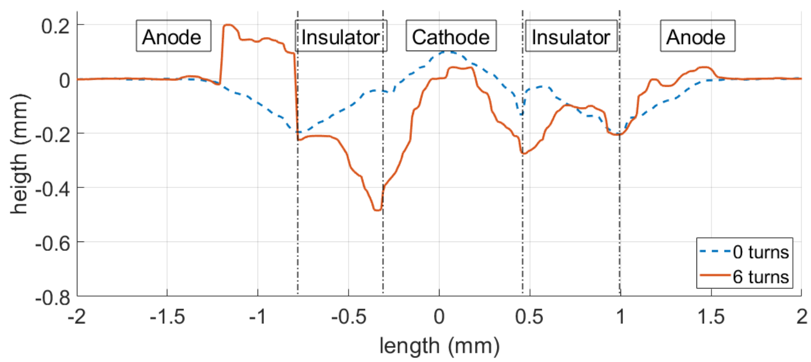

Figure 10. Laser profilometry results for conical alumina insulator, operated at 40 A peak discharge current, case showing the anode-insulator-cathode surface. 0 and 6 turns.

C. Conical boron nitride insulator, 40 A peak discharge current

The thruster failed with a short circuit after 11.75 turns. Photographs of the thruster surface are shown in Fig. 11. Profilometry results of the thruster surface is provided in Fig. 12.

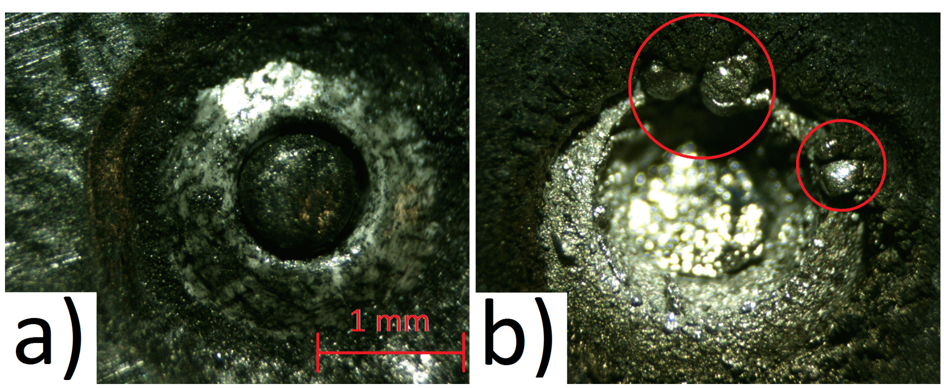

Figure 11. Photograph of a conical BN insulator, operated at 40 A peak discharge current, taken at 0 turns (a) and 11.75 turns (b). The images show a coaxial structure with the cathode in the center insulator in the middle and metal anode.

Compared to the conical alumina insulator, the use of a conical boron nitride (BN) insulator doubled the lifetime of the thruster, terminating with a short after 11.75 turn. In this case there is significantly less deposition on the insulator, and the deposition appears smoother than the previous case. Failure occurs

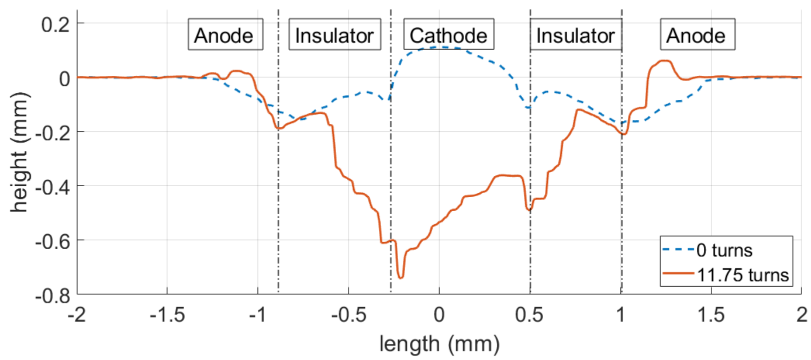

Figure 12. Laser profilometry results for conical BN insulator, operated at 40 A peak discharge current, showing the anode-insulator-cathode surface. 0 and 11.75 turns.

when the deposition on the anode surface grows to the point of blocking the line of sight of the plasma plume, leading to fast accumulation of material. This effect can be observed by the characteristic droplet shape of the deposition on the top right of Fig. 11. Figure 14 shows the profilometry of case C. We observe in the final result after 11.75 turns a very different outcome with respect to the previous cases. The cathode has receded by 0.7 mm and is now flat shaped. The insulator surrounding the cathode has significantly eroded to form an almost tube shaped structure. However, a double cone shape of the insulator is maintained near the anode interface. The BN insulator erosion process is preferable over that of alumina enabling significant reduction in metal deposition on the insulator. However, even this configuration is finally terminated by a short circuit.

D. Conical BN insulator, 60 A peak discharge current

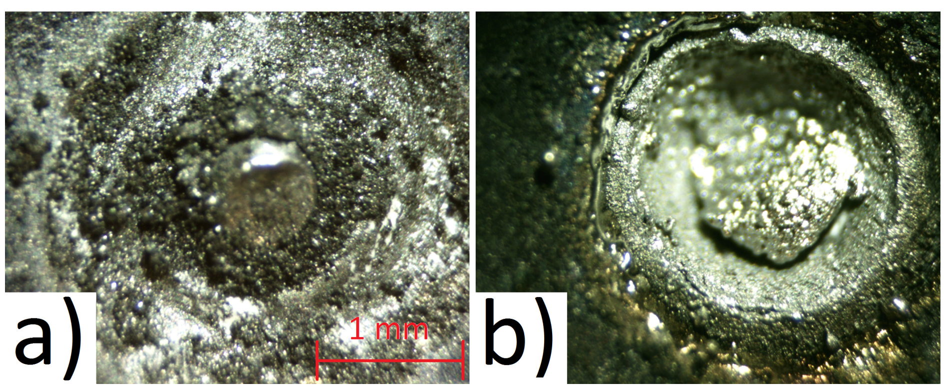

Figure 13. Photograph of a conical BN insulator, operated at 60 A peak discharge current, taken at 0 turns (left) and 15 turns (right). The images show a coaxial structure with the cathode in the center insulator in the middle and metal anode. The thruster was operated until the 15 turn goal was reached. This case had the same conical geometry and BN composition as case C, but the arc current was increased to 60 A. The arc pulse energy was maintained as before.

In this case the had the same conical geometry and BN composition, but the arc current was increased to 60 A. The arc pulse energy was maintained as before. The thruster was operated until the 15 turn goal was reached. When the thruster was inspected after the test no significant deposition was observed on the anode. Instead, the anode was found to be slightly eroded and its inner diameter has increased by $\approx$ 0.1 − 0.2 mm. Photographs of the thruster surface are shown in Fig. 13. Profilometry results of the thruster surface is provided in Fig. 14.

For firing duration of 90 seconds at 15 Hz and 0.2 J per pulse, the thruster erosion rate per firing cycle are:

- The BN erodes at the cathode contact points at a rate of $\approx$ 62 μ/turn

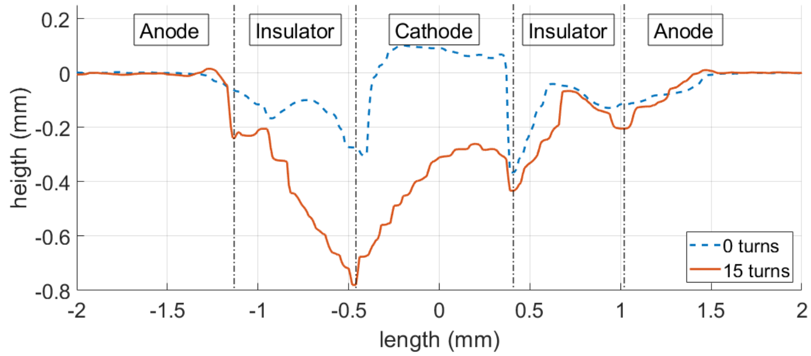

Figure 14. Laser profilometry results for conical BN insulator, operated at 60 A peak discharge current, showing the anode-insulator-cathode surface. 0 and 15 turns.

- The cathode is advanced by the feeding system 0.75 mm per turn. In addition we observe that the cathode recedes at the same rate as the BN with respect to the anode.
- Anode radial erosion rate at 60 A is ≈ 20 μm/turn; at arc current of 40 A no anode erosion is observed.

Table 1 summarizes the findings of the experimental campaign.

Table 1. Comparison between the experimental results of different ISF-VAT configurations

Case	Insulator geometry	Insulator material	Peak current (A)	Lifetime (turns)	End of life
A	Flat	Alumina	40	4.5	Short circuit
B	Conical	Alumina	40	6	Short circuit
C	Conical	Boron nitride	40	11.75	Short circuit
D	Conical	Boron nitride	60	15	Manual

Each of the changes led to an improvement in lifetime, but only the combination of all the factors prevented failure by short circuit.

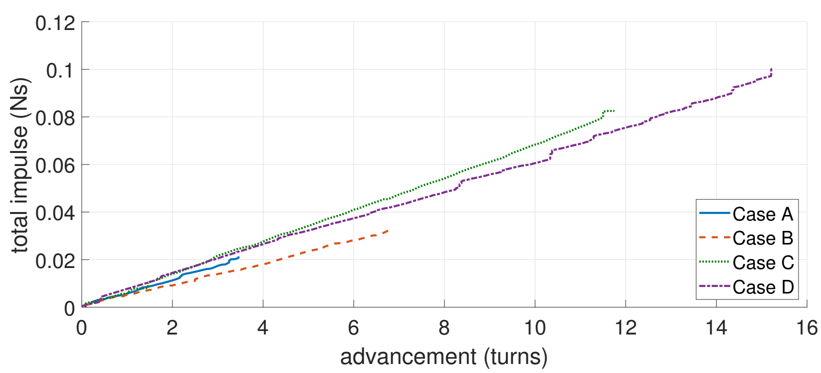

Figure 15. Total impulse provided as a function of cathode advancement. Each turn is 0.75 mm of cathode advance.

As the thrust is being measured and recorded continuously during the life time test, these data allow us to calculate the total impulse obtained in each case. Figure 15 shows the total impulse accumulated over time for a cathode mass feeding rate of 1.3 μg/s (62 μm per cycle, 1/12 turn). The total impulse increases proportionally with the cathode mass being processed, indicating that a constant thrust performance is being maintained.

IV. Conclusion

It was found that thruster lifetime is very sensitive to insulator geometry, insulator material and arc current. We succeeded in determining a configuration capable of reaching steady state in a repeatable manner. From these results we can conclude that the ISF-VAT can operate for long duration. During its operation the electrodes and insulator are eroded but at different rates. Assuming that the feeding mechanism is unlimited the thruster lifetime is mostly determined by the length of the insulator. A 4 mm long insulator will be capable of sustaining up to 150 turns, achieving a total impulse of 1-2 Ns.

References

[1]I. Levchenko, K. Bazaka, Y. Ding, Y. Raitses, S. Mazouffre, T. Henning et al., Space micropropulsion systems for cubesats and small satellites: From proximate targets to furthermost frontiers, *Appl. Phys. Rev.***5**, 011104 (2018).

[2]J. Mueller, R. Hofer, and J. Ziemer, Survey of propulsion technologies applicable to CubeSats, *paper presented at the Joint Army-Navy-NASA-Air Force (JANNAF) Conference*, Colorado Springs, CO, 2010.

[3]B. Jttner, Cathode spots of electric arcs, *J. Phys. D Appl. Phys.***34**, R103 (2001).

[4]I. Beilis, State of the theory of vacuum arcs, *IEEE Trans. Plasma Sci.* **29**, 657670 (2001).

[5]I. Beilis, Vacuum arc cathode spot grouping and motion in magnetic fields, *IEEE Trans. Plasma Sci.* **30**, 21242132 (2002).

[6]M. Keidar, I. Beilis, R. L. Boxman, and S. Goldsmith, 2D expansion of the low-density interelectrode vacuum arc plasma jet in an axial magnetic field, *J. Phys. D Appl. Phys.* **29**, 1973 (1996).

[7]M. Keidar, J. Schein, K. Wilson, A. Gerhan, M. Au, B. Tang et al., Magnetically enhanced vacuum arc thruster, *Plasma Sources Sci. Technol.* **14**, 661 (2005).

[8]I. Kronhaus, M. Laterza and A. R. Linossier, "Experimental Characterization of the Inline-Screw-Feeding Vacuum-Arc-Thruster Operation," *in IEEE Transactions on Plasma Science*, vol. **46**, no. 2, pp. 283-288, Feb. 2018. doi: 10.1109/TPS.2017.2776839

[9]I. Kronhaus, M. Laterza, and Y. Maor, Inline screw feeding vacuum arc thruster, *Review of Scientific Instruments*, **88**, 4, 043505, (2017), doi: 10.1063/1.4979706

[10]I. Kronhaus, Inline screw feeding vacuum arc thruster, *Israel Patent* 246250, Jun. 2016.

[11]B. Seifert et al., Verification of the FOTEC N thrust balance at the ESA propulsion lab, *in Proc. 34th IntμN Electr. Propuls. Conf.*, Kobe, Japan, Jul. 2015, IEPC paper 2015-258.